Blast Instrumentation for Lethality Assessment

Leo R. Gauthier Jr., John M. Klimek, Louis A. Mattes, Christopher L. Eddins, Angela L. Barrios, Dale E. Clemons, and Robert F. Walsh Jr.

A blast initiation detector (BID) was developed for use on Lance and Hera targets to detect the first light from fragmenting warheads. The measured time of first light, in conjunction with the measured time of first fragment impact, provides a method for computing the standoff distance. The standoff distance is a key measure of interceptor performance. A high-speed sled test afforded an opportunity to demonstrate and validate the BID/hit panel standoff measurement for the first time under conditions of known geometry with a moving warhead. The BID/hit panel standoff distance estimate was in agreement with the known geometric standoff distance to within approximately 2%. Lessons learned from the BID are being used to develop a blast position detector that measures the time and spatial location of the blast.

INTRODUCTION

APL has provided target-based instrumentation for ballistic missile intercept tests for several years. Increasing support for missile defense systems has fostered the development of target-based technology that is needed to measure interceptor performance. During the early 1990s, target-based instrumentation, referred to as hit panels, was made at APL to detect the arrival time of the damaging fragments from detonating warheads. Early work culminated in the successful Developmental Test Round-1A intercept in 1997. Hit panels on the target clearly showed the first fragment impact location and the damage propagation pattern.

Another instrument, known as a blast initiation detector (BID), was developed at APL for use on Lance targets and was more recently extended for use on Hera targets, which are used in Standard Missile-2 Block IVA interceptor tests. The BID is an electro-optical instrument that can rapidly detect the first light from the warhead explosion. The detection of first light provides a temporal reference point for the warhead event within the target telemetry. More significantly, BID data can be used with hit panel impact data to compute standoff distance, a key measure of interceptor performance. Figure 1 illustrates the concept. The main point is that by measuring the fragment travel time, the standoff distance can be computed from assumed fragment speeds.

The BID for the Hera target was developed concurrently with testing and analysis. The Electronic Systems Technology Team of the Aeronautical Science and Technology Group within the Research and Technology Development Center led the development effort. Testing centered on the use of the Avery Advanced Technology Development Laboratory (AATDL) cell 4 aerothermal test facility. During wind tunnel testing,

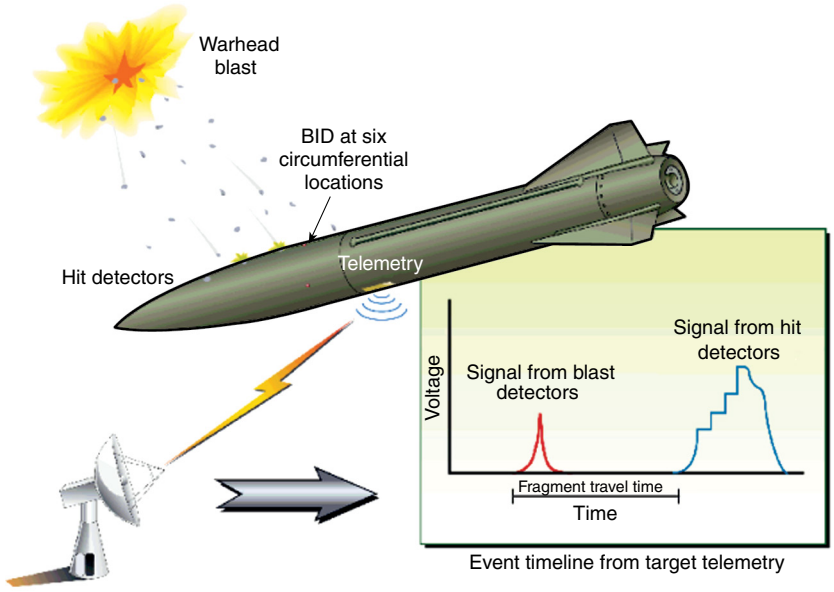

Figure 1. Estimation of the blast initiation detector (BID) standoff distance. The time difference between BID response and the first fragment impact from the hit detectors provides a means of estimating standoff distance from known characteristic fragment velocities.

the optical fiber design performance was validated under realistic aerothermal loads. The optical fibers were also tested to the point of failure to gain insight into the failure mode. The BID analysis centered on the development of a mathematical model of the electro-optical blast/BID system. The model was used to guide the design to ensure microsecond response times and limited shot-to-shot response time variability. Rapid response with limited variance is necessary to ensure that the BID detection is telemetered out before the target is destroyed and to limit the uncertainty introduced during the standoff distance computations.

After development was completed, five production units and one sled test unit were installed into the targets. During the sled test, the BID detected the warhead burst in less than 10 μs. The BID data were used along with hit panel data on the same target to compute the standoff distance. The computed standoff was within approximately 2% of the known geometric

GLOSSARY

The following terms are used in this article. Definitions and nomenclature are provided to remove confusion arising from alternative interpretations of the concepts and to provide a point of reference for the definition of parameters.

Blast initiation detector (BID). A target-based system of optical detectors and electronics that detects the first light from the warhead to provide a temporal reference point for the target telemetry. The BIDs for the Hera and Lance targets were developed by APL.

BID electronic latency (τ_{EB}). The time delay associated with the propagation of the signal through the BID electronics and the cable to the telemeter.

BID latency (τ_B). The time delay between the occurrence of the first fragment motion (first light) from the warhead and the first registration of this event in the telemetry stream.

BID latency variance (σ_B^2). The expected value of the square of the difference between the actual BID latency and the average BID latency. It is a measure of the variability in BID response times.

Blast position detector. An electro-optical system used to determine the location of the blast in target-centric coordinates. It is in development at APL.

Detonation latency. The time between when the warhead is instructed to detonate and the time of first fragment motion (or first light).

Diagnostic latency (τ_d). The time delay between the occurrence of the first fragment motion (first light) from the warhead and the second registration of this event in the BID telemetry stream that corresponds to the fiber with the second-best FOV. This may occur or it may not occur at all, depending on the blast location. These additional BID data may be used to infer some degree of blast orientation.

Electromagnetic latency (τ_L). The time delay associated with the propagation of the light from the warhead to the closest-response fiber aperture.

Geometric latency (τ_X). The time delay associated with the geometry of the blast-to-fiber interface during which the signal rises to a detectable level. The geometric latency depends on the distance from the closest-response fiber to the blast and the angle between the fiber aperture and the blast. This is the largest component of BID latency.

Hit detector. The hit detector is a system that detects impact fragments on the target vehicle. The hit detector on the Hera target is implemented by ITT Industries, Inc.

Hit detector electronic latency (τ_{EH}). The time delay associated with the propagation of the signal through the hit detector electronics and the cable to the telemeter.

Hit latency (τ_H). The time delay between when a fragment impacts the target vehicle and when the event is registered in the telemetry stream.

Standoff distance. The distance from a reference point on the target to the origination point of impact fragments on the outer surface of the warhead at the instant of first fragment movement (equivalent to first light).

Telemeter latency (τ_T). The time delay between the arrival of a signal at the telemeter and the time when the signal is actually time-stamped.

standoff distance. This was the first time the BID/hit panel technique was used to compute standoff in a moving warhead test. The BID lessons learned are being used to develop a stand-alone blast position detector that can resolve blast position and initiation time independently of hit panel data or fragment velocity uncertainties.

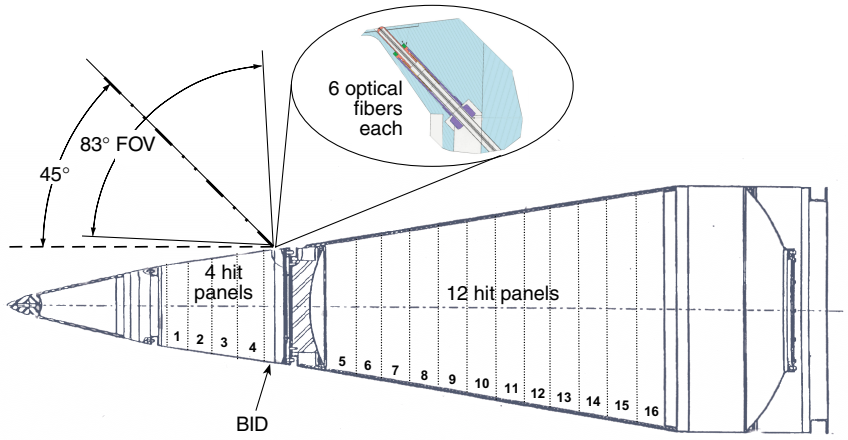

Figure 3. Target-based instrument locations are shown for the Hera target. The BID is located near the aft bulkhead of the forward section. The optical fibers look forward at 45° into the anticipated blast zone with an 83° field of view (FOV). Sixteen hit panels cover the payload and forward sections.

BID DESCRIPTION

The Hera BID is composed of an electronics module that connects to six optical fibers. The optical fibers connect the external environment of the target vehicle to the electronics module and detect the first light from the warhead. A block diagram of the system is shown in Fig. 2. The optical fibers are made of multistranded borosilicate glass fibers enclosed in a 20-in. stainless steel shroud. The high numerical aperture of the glass provides a wide field of view (FOV) to detect blasts over a wide range of various locations. The optical fibers can withstand temperatures as high as 1200°F on the exposed distal tip. The BID and other instruments are installed aboard the target vehicle as shown in Fig. 3. The optical axis of each forward-looking optical fiber makes a 45° angle with the target vehicle axis. The FOV of the six fibers covers the anticipated blast zone so that at least one fiber can see each expected blast location. Figure 4 illustrates the estimated blast region for a 10-μs response time.

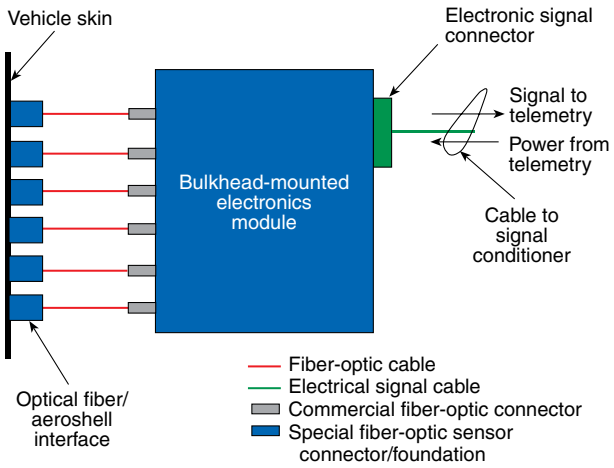

Figure 2. Block diagram of the BID. The BID is a target-based system of optical detectors and electronics that detects the first light from a warhead explosion. The first light provides a temporal reference point for the intercept in the target telemetry.

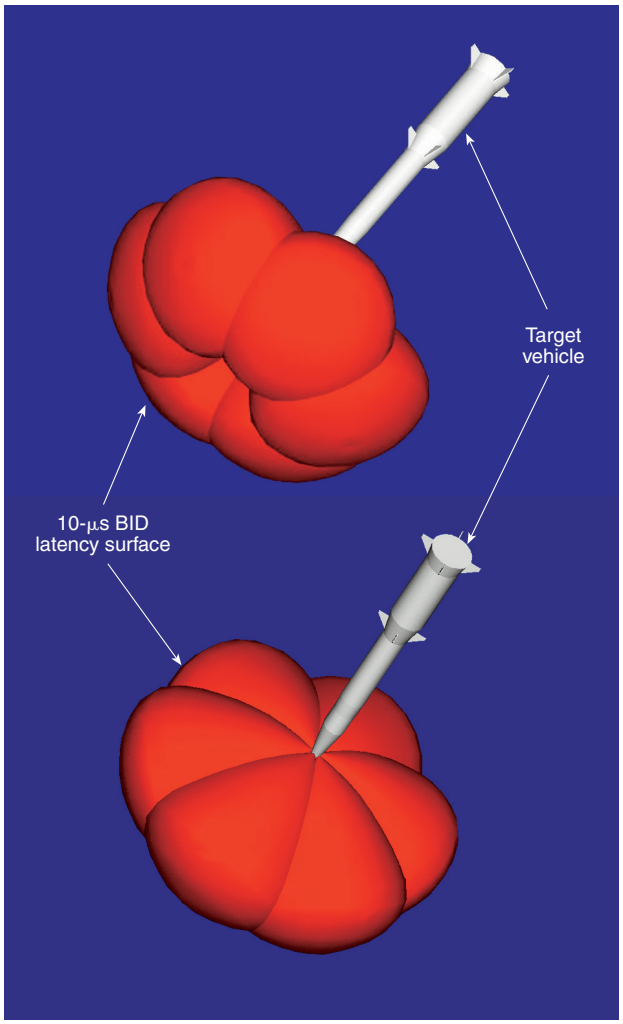

Figure 4. A three-dimensional latency surface illustrates the blast region with optimal latency. The lobes correspond to the six optical fibers. Blasts that detonate within the region enclosed by the surface will be detected in less than 10 μs.

WIND TUNNEL TESTING

Wind tunnel testing was used to address the optical performance concerns about high temperatures on the exposed fiber tip.[1] Figure 5 illustrates the air penetration of the exposed distal tip of a fiber. The test hardware was fabricated to simulate the BID optical/aeroshell environment upon reentry. The circular plate in Fig. 5b shows the instrumented portion of the wind tunnel test hardware and is representative of a small section of the aft bulkhead of the forward section of the target vehicle. The materials and the design were best-effort duplicates of the actual flight hardware. The test fixture was instrumented as shown in the infrared view of Fig. 6 and installed into the AATDL cell 4 wind tunnel test facility. During the tests, two laser beams were toggled onto the optical fiber at two different angles of incidence, approximately 25° and 35° off-axis. Temperatures, pressure, qualitative infrared thermal images, schlieren images, and relative optical throughput were recorded during four tests. The schlieren images revealed the shock structure at the BID fiber distal tip protrusion. The infrared images showed the basic heating trend of the test fixture. The optical fibers of the BID benefit from the cooling effect of the thicker material in the bulkhead. Figure 7 is an inverse color image of the laser beams that were incident on the optical fiber. The laser beams became visible in the wind tunnel water vapor

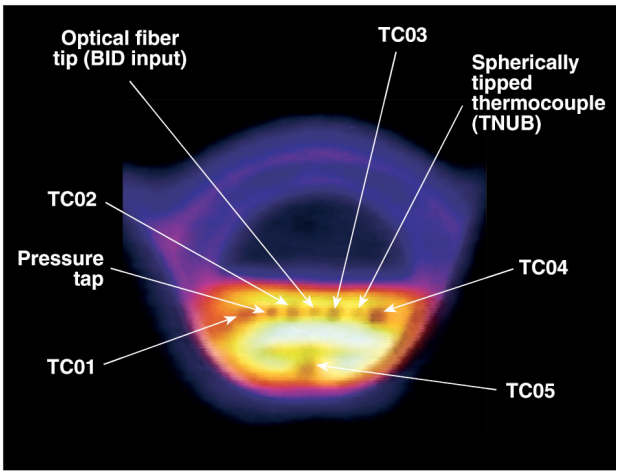

Figure 6. Infrared image of the BID wind tunnel test hardware. Shown are the locations of the five plate thermocouples (TC01 through TC05), the protruding tip thermocouple (TNUB), the BID optical fiber, and the pressure tap. The features are distinguishable in the infrared image. The cooling evident in the upper portion of the image is a result of the thicker bulkhead material.

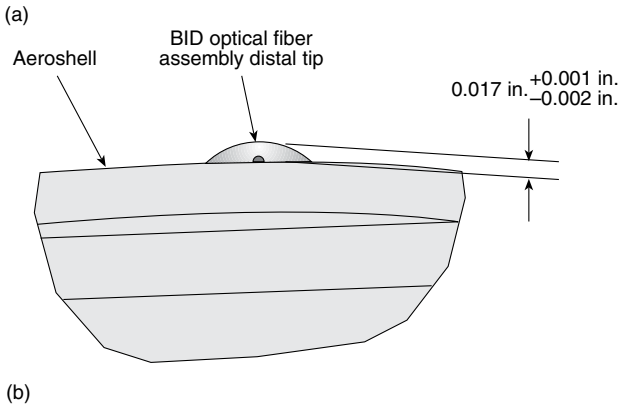

Figure 5. The test hardware used in wind tunnel tests at the AATDL was used to simulate the part of the target vehicle where the BID optics penetrate the airstream. The penetration depth was minimized to reduce aerothermal loads. (a) Diagram of the test hardware looking aft and (b) oblique view.

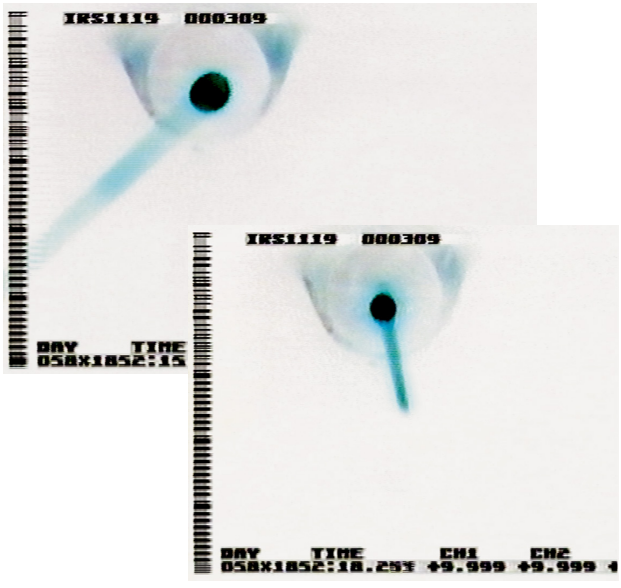

Figure 7. Inverse color laser beams are rendered visible by water vapor. The hydrogen torch used to heat the air in wind tunnel tests adds water vapor to the airstream. The water vapor makes the laser beams visible during some tunnel conditions.

that was added to the airstream by the hydrogen torch used to heat the air. Other data are discussed next.

Test 1

The first wind tunnel test occurred on 10 February 2000. The total pressure was 488 psia (lb./in.^{2} absolute), and the total temperature was 1406°R. The objective of this test was to provide the basic proof of concept that validated the design of the fiber/aeroshell interface. The optical fiber tip protruded into the boundary layer to a depth of 0.014 in. The skin temperatures gradually approached 800°F during the 3-min exposure. The optical throughput and FOV remained constant. The temperature of the protruding distal tip was only a few degrees higher than the hottest skin temperature. By minimizing the protrusion distance, very little temperature increase was induced by the boundary-layer protrusion.

Test 2

During the second test, the protruding tip was extended from 0.014 to 0.018 in. normal from the surface of the plate. The increased protrusion was selected to afford some tolerance for thermally induced expansion and contraction of target vehicle components while preserving the required FOV. The same optical fiber was reused from the first test. The tunnel conditions were more severe than in the first test, and an attempt was made to thermally shock the protruding fiber similar to what would be expected on reentry. The total pressure was 444 psia, and the total temperature was initially 2654°R. As shown in Fig. 8a, the distal tip temperature exceeded 1200°F for a few seconds. The thermocouple signals correspond to TC01 through TC05 and TNUB according to the locations shown in Fig. 6. The optical signal was the result of two laser beams that alternately strobed the BID optical fiber interface at different angles of incidence. The upper optical signal for each test corresponds to the 35° off-axis laser, and the lower optical signal corresponds to the 25° angle. As the tunnel conditions were relaxed to a total pressure of 479 psia and a total temperature of 1296°R, the surfaces cooled and then reheated, gradually approaching 800°F. As in test 1, the optical throughput and FOV were preserved for the full exposure time. However, the increased protrusion distance was evidenced by the temperature augmentation of the tip relative to the skin. In this test, the tip peaked as much as 200°F warmer than the skin and ended up approximately 50°F warmer for the duration of the test.

Test 3

The thermal conditions were substantially worsened during the third test. The laser on-times were reduced from 5 s down to 3 s to ensure that data were acquired for at least several transitions under the more severe conditions. The same optical fiber was again used. The intent during this test was to induce optical failure of the fiber. The total pressure of the tunnel was 282 psia, and the total temperature was 2576°R. The optical interface failed approximately 50 s into the test. This failure was followed by a gradual ramping of the baseline optical signal for about 20 s until the wind tunnel conditions were relaxed. The measured protruding tip temperature was actually lower than measured skin temperatures during this test, which was attributed to nonsymmetrical heating profiles within the tunnel under the stated run conditions. Subsequent inspection of the test fixture revealed that the sudden loss of optical throughput was caused by the melting of solder that was used to bond thermocouple TC05 to the test fixture. The solder melting temperature was 1105°F, consistent with temperatures recorded on the test fixture skin surface. A track of ablated material was seen from the location of thermocouple TC05 to the protruding tip of the optical fiber, and melted metal residue was evident on the fiber tip. The slow ramping signal measured after the abrupt loss of optical throughput was attributed

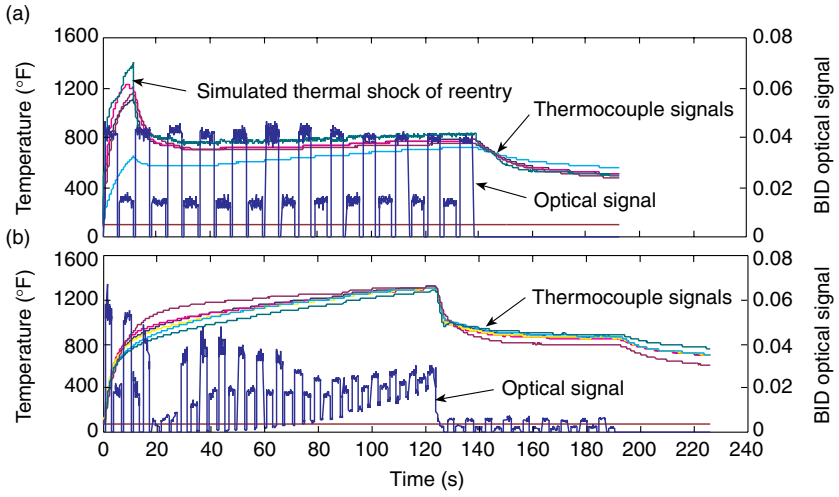

Figure 8. Comparison of good optical performance with optical failure. (a) Wind tunnel test data from test 2 showed excellent optical fiber performance. The temperature at the tip exceeded 1200°F during the simulated thermal shock of reentry. The optical throughput and FOV remained constant. (b) Test data from test 4 showed optical failure caused by small amounts of low-temperature epoxy in the exposed distal tip. After the tip melted, the optical throughput was reduced by ≈90%.

to the glowing molten material on the fiber tip. This signal quickly vanished when the tunnel conditions were relaxed to cool down. When the molten material was removed from the distal tip after the test, the intact ends of the glass fiber strands could still be clearly seen under a microscope.

Test 4

The fiber manufacturer had experienced great difficulty in reliably reproducing the fibers with the high-temperature epoxy used in the fiber from tests 1 through 3. In production, many fibers fractured during the polishing process. To increase yield in the first production batch, a small amount of low-temperature epoxy was added to the spaces between the 50-μm fiber strands; the surrounding epoxy was still all high-temperature material. There were concerns that the addition of the low-temperature epoxy would compromise the thermal survivability of the fiber tips. These concerns were substantiated in test 4.

Test 4 was a repeat of test 3 to optical failure with a fiber that used a small amount of the lower-temperature epoxy. Data shown in Fig. 8b indicated that the optical throughput was lost within 20 s. This was followed by a gradual exponential rising of the background optical signal (when the lasers were off) and erratic optical throughput for the next 105 s. This background rise was followed by immediate loss of background optical signal on transition to tunnel cool-down, with optical throughput reduced to approximately 10% of the original. Subsequent disassembly of the distal tip showed that the glass in the tip had melted. The exponentially rising background was attributed to the glowing/burning tip. A comparison of the optical performance between Figs. 8a and 8b clearly illustrates the optical failure during test 4. The main conclusion from test 4 was that no low-temperature materials could be tolerated in the optical fiber distal tip.

After these test results were interpreted, APL went back to the fiber manufacturer and jointly solved the production yield problem by the following process changes:

- Use of only high-temperature epoxy, but with a reduced aluminum particle size to improve fiber-to-fiber interstitial bonding
- Use of a syringe rather than an open mixing pot to hold mixed epoxy and increase pot life
- Use of a hand pick to push epoxy into the fiber-to-fiber interstices
- Use of a grinding/polishing process, with reduced particle sizes on the polishing apparatus to reduce fiber jarring and fracturing

The final production fibers were identical to those used during tests 1 through 3, except for the manufacturing process changes noted.

BID LATENCY ASSESSMENT

The blast time is needed in conjunction with warhead fragment velocity and hit location data to compute the standoff distance of the warhead during the endgame analysis. Any latencies or delays associated with the detection processes must be understood so that the timing data reported by the telemetry can be correctly interpreted. This section details the timing latency assessment for the BID that is planned for use aboard Hera target vehicles during flight interceptor demonstration tests.

The BID latency is the time delay between the occurrence of the first fragment motion (first light) from the interceptor warhead and the first registration of this event in the target telemetry stream. In general, the BID latency is a function of many optical and electronic variables and the geometry between the BID detection fibers and the warhead blast. Since the cabling delays are approximately equal and common to both the BID and the hit panel instruments, they are irrelevant to the standoff distance computations.

For the Hera target application, six forward-looking fibers are equally spaced around the circumference of the forward section and are used to receive the blast signal. Since the value of the BID latency can be corrected for if known, it is the variance and, therefore, the standard deviation of the BID latency that is minimized by design. The six-fiber coverage, the fiber orientation, and the alternating current (AC) coupling approach were selected to minimize the variance of the BID latency within the constraints imposed by available fiber mount positions.

The analysis indicates that worst-case BID latency will be approximately 25 μs and that the BID latency will be less than 10 μs for greater than 98% of intercept scenarios where no direct interceptor contact is involved.[2] In addition, new optical fibers may further reduce the response time.

The analysis indicates that the timing uncertainty associated with the BID and hit panel signals will introduce a very small uncertainty into the standoff distance estimation. The uncertainty in the BID timing is small enough so that the largest error terms in the standoff distance computations are in the fragment velocity uncertainty. In practice, the BID latency should be small enough to ignore for most purposes.

Target-Centric Coordinate System

A three-dimensional rectilinear coordinate system was defined with respect to the target vehicle and was used for all blast simulations. The positive z axis coincides with the axial centerline of the target vehicle and passes through the nose. The six BID fibers (1–6) are located slightly forward of the origin, as shown in Fig. 9.

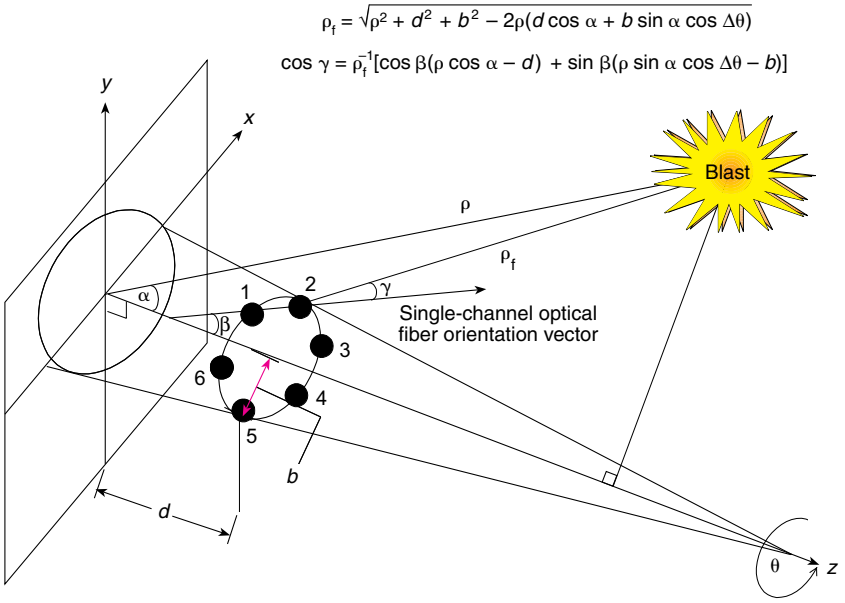

Figure 9. Target-centric coordinate system geometry. The distance from the blast to the optical fiber ρ_f and the cosine of the off-optical-axis viewing angle γ determine the BID geometric latency.

Defining β to be the angle between the target axis and the optical fiber axis, expressions for the distance from the blast to the optical fiber ρ_f and the cosine of the off-optical-axis viewing angle γ are provided in Fig. 9.

For the Hera application, 200 simulations of the endgame interception event were run to provide a representative ensemble of endgame blast locations with respect to the target vehicle.[3] The significant data in these simulations were the α and ρ values. For analytical purposes, $\Delta\theta$ was treated as a variable with a uniform distribution over the range of $(-30° < \Delta\theta < 30°)$ for each α and ρ value. The fiber was oriented at $\Delta\theta = 0$. For each of the 200 α and ρ pairs, 31 values of uniformly distributed θ were used to provide a representative set of 6200 blast locations. The β value for the Hera target is 45° and was selected to minimize BID latency variance given the constraints of available mounting locations and fiber bend radius. The value of d is 0.77 ft, and that of b is 0.70 ft (see Fig. 9).

It is clear from the simulated intercepts that the missile may come in contact with the target vehicle prior to detonation. On the basis of the representative set of blast locations and a spherical warhead approximation, a probability exists of sustaining a direct warhead intercept. In these intercept scenarios, the hit detector signal may occur in the absence of or prior to the BID signal. For this reason, the simulated blast locations corresponding to these intercept scenarios were removed from the data set for BID latency analysis.

Assumptions for Timing Analysis

The following simplifying assumptions were made for timing analysis:

- The fireball is modeled as a point source of light with an intensity rate of rise equal to that measured during a prior sled test. The point-source assumption implies that the incident radiation falls off as the inverse square of the distance. For blasts on the periphery of the FOV, real fireballs will likely reduce realized BID latency as a result of increased optical energy within the FOV. For blasts occurring in direct line of sight of a fiber, the spatial distribution of the energy off the optical axis may slightly increase the response time.
- Measurements of the fireball diameter indicate that the spatial growth of the fireball is less significant than the growth in the radiant output during the early stage, although both effects undoubtedly contribute to the rising energy at the fiber aperture. Therefore, it is necessary to be able to detect each blast location directly, even at the extreme angles of the FOV. The BID does not wait for the fireball to "propagate" into the FOV of a fiber.
- For purposes of analysis, statistical variations in warhead radiation intensity from blast to blast were not considered. On the basis of previous sled test data, shot-to-shot variability is significant and will contribute to the spreading of the latency distribution.
- The BID has six fibers that attach to six amplifiers within the BID box. For purposes of analysis, BID channel-to-channel variations were ignored. Channel-to-channel variations, including fiber coupling tolerances (alignment, transmissivity) and amplifier gain tolerances, were not addressed. Electronic component tolerances were also not addressed.
- The numerical aperture of the fiber remains fixed at 0.66 over the temperatures experienced by the fiber. This was substantiated by wind tunnel testing at the AATDL.
- The hit detector latency is very small, less than 200 ns. This was verified by the Hera target hit panel designer.
- A manufacturer-provided photodiode curve was used to convert blast spectral data to voltage.
- Measured test data from one optical fiber with one photodiode were used to characterize the off-axis attenuation of light.

AC versus DC Coupling

In general, the optical signal from the blast can be coupled into the BID by either direct current (DC) or AC coupling. In DC coupling, signal registration occurs when the incident light intensity exceeds a preset level. In AC coupling, the signal registration requires two conditions: (1) the rate of rise of the incident light intensity must exceed a threshold level, and (2) the first stage cannot be saturated by the ambient light.

The five identified possible sources of interference with AC coupling are the following: (1) cloud shadowing, (2) intercept shadowing, (3) intercept reflections, (4) ground reflections, and (5) glow rise. In cloud shadowing, the target passing out of a cloud shadow could, in general, register a BID event as the Sun rapidly comes into view. This is not likely to be a problem at intercept altitudes. Intercept shadowing occurs when the target passes out of the shadow cast by the incoming interceptor. This is also a very low-probability event, given the required orientation of the Sun, interceptor, and target system. Intercept reflections can occur when the sunlight reflects off the target and becomes incident on the BID fibers. Similarly, ground reflections, such as those from a lake, could be bright enough to register a BID response. Both types of reflections are considered very low-probability events in the time frame of interest (the 10-μs detection window). Glow rise is caused by the rise in incident radiation on the BID fibers as a result of the aerothermal heating of external vehicle surfaces as they come into view. The target glow and the interceptor glow both contribute to this noise source. The rate of glow rise should be well below the threshold rate of rise. The BID threshold rate of rise also limits the likelihood of the other events causing a false BID signal. As a point of reference, a camera flash bar with a rise time of 2 ms is too slow to be seen by the Hera BID. On the basis of this reasoning, the probability of false BID registration causing confusion during the endgame is very low with AC coupling.

The most likely interference source from DC coupling is the Sun. An arena test at the Naval Surface Warfare Center/Dahlgren Division on 26 August 1999 demonstrated that DC coupling with a threshold set high enough to exclude Sun interference can introduce excessive latency (215 μs) and, more importantly, excessive BID latency variance.[4] The DC-coupled Lance target BID latency is still acceptably low as a result of the use of larger optical fibers and further aft mounting positions.

There are numerous advantages to using AC coupling for the Hera target BID. Since the AC-coupled BID has no significant interference sources, the gain in the electronics may be set much higher. This effectively reduces the detection threshold and the latency for all blast locations and leaves the bulk of the standoff distance uncertainties in the warhead fragment velocity.

Hera BID Latency

The BID latency is the sum of four latency effects: (1) electromagnetic τ_L, (2) geometric τ_X, (3) electronic τ_{EB}, and (4) telemeter τ_T latency:

$$\tau_B = \tau_L + \tau_X + \tau_{EB} + \tau_T \ .$$

The electromagnetic latency is less than 20 ns for all typical standoff distances and is dependent on the distance from the blast to the fiber. The electronic latency is less than 200 ns. The telemeter latency stems from the onboard 5-MHz free-running oscillator on the target vehicle. The telemeter latency is nominally 100 ns, with a maximum of 200 ns.

The BID latency is dominated by the geometric latency. The geometric latency τ_X is caused by two effects: (1) the distance of the blast from the fiber, and (2) the off-axis attenuation as a result of the numerical aperture of the fiber and the cosine projection factor.

A first-order estimate of the geometric latency, and therefore the BID latency τ_B, is expressed as

$$\tau_B \approx \tau_X = RC \ln[1 - S^{-1} I^{-1} \rho_j^2 F^{-1}(\gamma)]^{-1} \ ,$$

where

S = a system composite gain parameter,
I = the warhead intensity rate of rise,
F = the optical fiber fall-off function, and
RC = the time constant associated with the AC coupling.

The first-order solution was used to validate a more comprehensive model based on the solution to a differential equation.

From solutions to the more comprehensive model, the worst-case geometric latency τ_{worst} was computed. Note that γ_{worst} is not the worst fiber viewing angle but that the combination of (ρ_{worst}, γ_{worst}) yields the worst geometric latency. The estimate of the worst-case latency, using measured blast data from a prior sled test, was 24.9 μs for τ_{worst}. The expected value of the BID latency is less than 10 μs. New optical fibers will reduce the latency even further.

Hit Latency

The hit latency τ_H is composed of two elements, electronic latency τ_{EH} and telemeter latency τ_T. Cable propagation latency is common to both the hit panels and the BID and does not need to be considered. The telemeter latency is the same as that for the BID. According to the Hera target hit panel designers, the hit detector electronic latency is less than 200 ns.

Endgame Timeline

Figure 10 illustrates the timeline associated with the endgame events *E*. If T_B and T_H are the time stamps in the telemetry stream associated with the first BID event and the first fragment hit event, respectively, then the best estimate of the actual fragment travel time T_F can be computed:

$$T_F = [T_H - E(\tau_H)] - [T_B - E(\tau_B)],$$

where the expected values are used for the BID and hit panel latencies.

System Standard Error

The BID/hit panel system timing standard error σ_s is the root-sum-square uncertainty in T_F and is expressed here as the root-sum-square of the standard errors associated with the BID and the hit detector. The root-sum-square value is reasonable because both measurements are performed independently:

$$\sigma_s = \sqrt{\sigma_B^2 + \sigma_H^2} \quad .$$

Analysis indicates that the system timing error introduced by the BID and hit panel latencies is dominated by the BID geometric latency and is approximately 2.4 μs.

The system timing error is very small and not significant for endgame analysis interpretation. Thus it is clear that the bulk of the error in the standoff distance computations will arise from uncertainty in the fragment velocities and not in the target-based instrumentation. Even if the actual geometry represented a worst case for BID geometric latency, the uncertainty in standoff distance because of BID timing would be less than 1 ft; and because worst-case geometric latency occurs at the greater standoff distances, this is a reasonable worst-case estimate of the standoff distance uncertainty caused by the instrumentation.

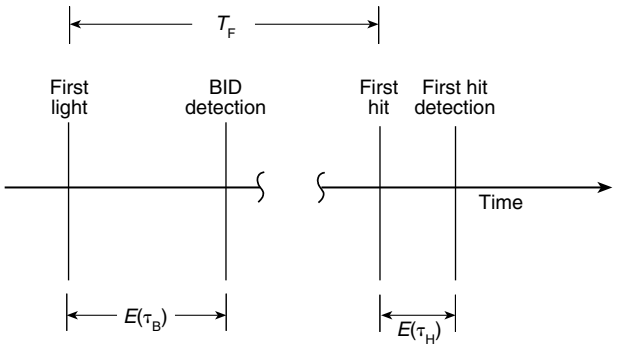

Figure 10. Endgame timeline. The four events of significance for estimating the fragment time of flight are (1) first light emanates from the exploding warhead, (2) BID detects the first light, (3) first fragment from the warhead makes impact on the target hit panel, and (4) first impact is detected by the target hit panel. By using instruments with fast response times, the fragment travel time T_F is measured and standoff distance can be estimated.

Ramifications for Endgame Analysis

The computed T_F and σ_s timing parameters should be considered to be best estimates of BID performance, based on available data. The BID latency model will be refined as experience with the system is gained.

It may be possible to use second BID event data to further resolve the blast orientation. For this reason, the latency of the second BID signal is called the diagnostic latency τ_d. The diagnostic latency may be used to validate or refute the computed endgame geometry based on the first BID event.

At least two known time delays and associated uncertainties exist that would have to be accounted for if the target and interceptor time bases were ever to be correlated: (1) T_F does not include the warhead detonation latency, and (2) according to the telemetry interface designer, there is a delay of approximately 3 μs that is associated with changing from preintercept telemetry to postintercept telemetry aboard the target vehicle.

There are two corrections for the standoff distance estimation as well: (1) the fragment hit location will be different from the origin of the target-centric coordinate system, and (2) the physical size of the warhead should be accounted for since the fragments do not, in fact, propagate from the center.

SLED TEST RESULTS

A BID in the forward section of the target was used to detect the blast signal during a recent sled test.[5] The test geometry is shown in Fig. 11. The BID response time was measured independently in this test by using two external optical fibers attached to the two BID channels on the side of the target away from the warhead. The external optical fibers were placed for ideal viewing of the warhead's first light with essentially zero latency. The measured BID response time, referenced from the detection of first light through the external fibers, was 9.4 μs. Figure 12 shows the blast at the moment of detonation.

Evaluation of test data demonstrates the utility of computing the standoff distance based on the BID measurement of warhead flash and hit panel reports of fragment impact. The agreement between the computed standoff distance and the known geometrical standoff distance for the sled test was approximately 2%. The difference can be explained by the use of an assumed fragment velocity value that was extracted from the probability distribution of actual fragment velocities. There could not be such close correlation between the known standoff and the computed standoff without very small BID and hit panel response times.

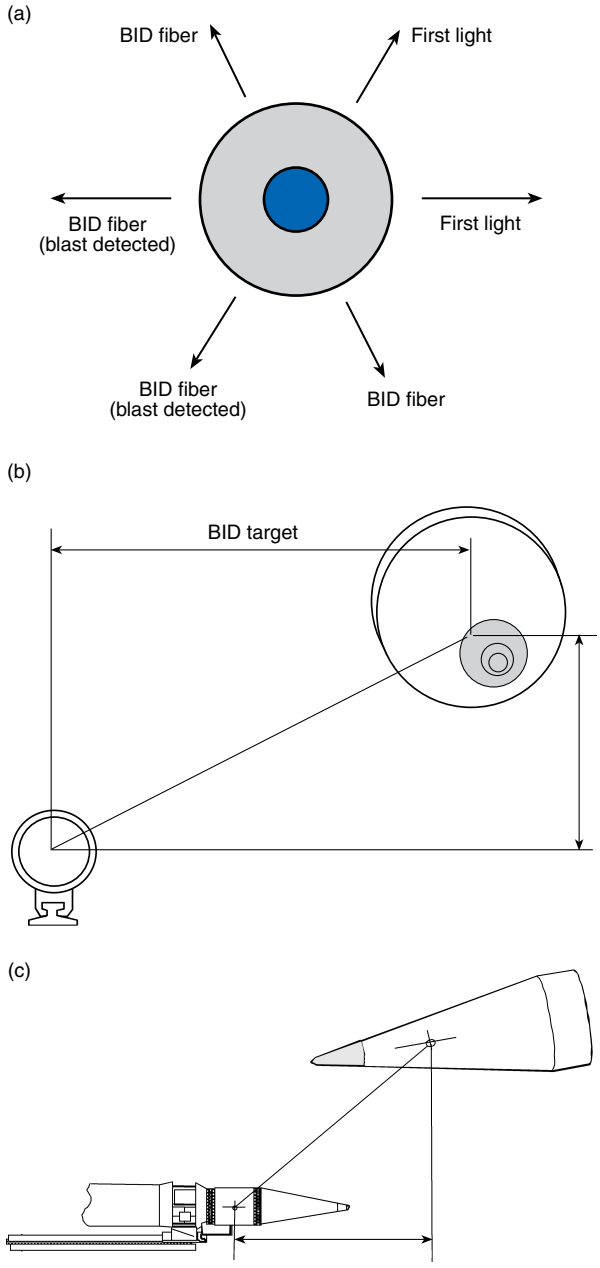

Figure 11. The sled test geometry shows the relative geometry of the target to the sled during the high-speed sled test. (a) Straight-on view of the target with BID fiber orientation, (b) straight-on view of the target and track, and (c) side view of the target and track. The two BID optical fibers that detected the blast are shown. The BID latency was measured by using two large external fibers attached to the BID channels on the shadow side of the target, labeled "First light." The external fibers were positioned for ideal viewing of the blast. The BID latency was measured to be 9.4 μs during the test.

Figure 12. This high-speed photograph shows the target with the BID as the warhead begins to explode.

CONCLUSIONS

Wind tunnel tests were performed to guide the design process and to provide a proof of concept of the optical fiber/aeroshell interface design. Test data indicate that temperatures experienced by the protruding distal tip are not significantly higher than the aeroshell skin temperatures and are within the thermal survivability envelope of the materials used.

From wind tunnel data from test 4, it was recognized that even small amounts of low-temperature epoxy in the distal tip of the optical fibers greatly impaired performance. On the basis of data from tests 1 through 3, the optical fiber/aeroshell interface that was designed for the BIDs and modified slightly for production withstood the simulated thermal environment during reentry for the required performance duration with little or no thermally induced loss of optical throughput or FOV.

By design, the Hera BID latency and its variance are limited to less than 10 μs for greater than 98% of the expected endgame scenarios where the warhead is not in direct contact with the target. From the timing latency analysis, it was determined that the timing latency of the BID would not be a significant factor in the overall standoff distance estimate. This was validated by the recent sled test data.

BID test experience has now demonstrated that the raw time-stamp data from the target instrumentation are sufficient to adequately resolve the standoff distance. The sled test demonstrated that the combination of BID and hit panel data can provide an effective tool for post-test lethality assessment.

REFERENCES

[1]Gauthier, L. R. Jr., Mattes, L. A., and Eddins, C. L., "Blast Initiation Detector Proof-of-Concept Wind Tunnel Testing of Optical/Aeroshell Interface," in *Proc. 2000 Missile Science Conf.*, Monterey, CA (7–9 Nov 2000), in press.

[2]Gauthier, L. R. Jr., and Klimek, J. M., "Blast Initiation Detector for Target Vehicles," in *Proc. 2000 National Fire Control Symp.*, Orlando, FL, Vol. 1, published on CD-ROM by Anteon Corp. (Aug 2000).

[3]Axenfeld, D. J., *Output Files for a Statistically Representative Set of Blast Locations Relative to the Target Vehicle*, JHU/APL TIMFUZ version 6.03L Simulation (3 Dec 1999).
[4]Cusick, R. T., Land, H. B. III, and Klimek, J. M., *HFD Arena Test Trip Report*, HFD-99-017, JHU/APL, Laurel, MD (30 Aug 1999).
[5]Gauthier, L. R. Jr., Barrios, A. L., and Clemons, D. E., *Validation of Blast Initiation Detector/Hit Panel Standoff Distance Measurement—Final Test Report*, ADS-01-010, JHU/APL, Laurel, MD (Feb 2001).

ACKNOWLEDGMENTS: The BID effort was sponsored by the Ballistic Missile Targets Joint Program Office, U.S. Army Space and Missile Defense Command. Special thanks are extended to Richard T. Cusick for his vision, John R. Coleman for programmatic oversight, Jim B. Kouroupis for aeroshell thermal predictions, Mike J. Neuenhoff for the cell 4 support, and the many others involved with the APL BID development effort. Other major contributors to the target instrumentation effort include Richard T. Cusick, Michael J. Byrne, Kenneth R. Grossman, Charles C. Rodeffer, and Jim B. Kouroupis.

THE AUTHORS

LEO R. GAUTHIER Jr. is a member of APL's Senior Professional Staff in the Research and Technology Development Center. He received a B.S. in electrical engineering from Boston University in 1986 and an M.S. in electrical engineering from The Johns Hopkins University in 1997. He is currently the Team Leader for Electronic Systems Technology in the Aeronautical Sciences Group. He has worked on the design of specialized instrumentation and systems in support of emerging problems of national interest, including missile defense. Mr. Gauthier supported the Arc Fault Detector and Continuous Thermal Monitoring programs for several years and led the systems engineering effort for the Virginia class AFD/CTM system. He was the Project Manager for the Blast Initiation Detector development effort for Hera targets. His e-mail address is leo.gauthier@jhuapl.edu.

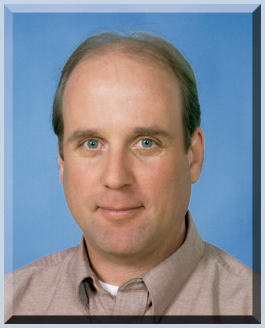

JOHN M. KLIMEK is a member of APL's Senior Professional Staff in the Research and Technology Development Center. He received a B.S. in electrical engineering from the University of Wyoming in 1988. As a member of the Electronic Systems Technology Team in the Avery Advanced Technology Development Laboratory, he has supported many design, analysis, and testing tasks in the area of specialized instrumentation. Mr. Klimek has a broad background in digital, analog, and optoelectronics design, and experience developing customized graphical user interfaces. Past efforts include the development of a prototype infrared scanning imager, along with printed circuit board and detector designs for the Continuous Thermal Monitoring Program. In the AATDL he led the effort to develop the rapid electronic prototyping capability. He is currently developing hardware and software for CONTOUR ground support equipment. His e-mail address is john.klimek@jhuapl.edu.

LOUIS A. MATTES is a member of APL's Senior Professional Staff and Supervisor of the Mechanical Systems Technology Section in RTDC's Aeronautical Sciences Group. He received a B.S. in mechanical engineering from The Johns Hopkins University in 1986. He joined APL in 1981 and has worked on many tasks involving the design, fabrication, and testing of advanced aerospace propulsion systems and related programs. Mr. Mattes is a member of the ASM International Materials Information Society. His e-mail address is louis.mattes@jhuapl.edu.

CHRISTOPHER L. EDDINS is a member of APL's Associate Professional Staff and is a systems/instrumentation engineer in RTDC's Aeronautical Science and Technology Group. He received a B.S. in electrical engineering from the University of Maryland, College Park, in 1995. Since joining APL in 1994, he has been an instrumentation/control engineer supporting tests in the Avery Advanced Technology Development Laboratory. His work also involves developing several instrumentation packages for use on a variety of flight vehicles. Additionally, Mr. Eddins has worked extensively on the development of the Continuous Thermal Monitoring Function of the Arc Fault Detector and Continuous Thermal Monitoring (AFD/CTM) Program. His e-mail address is chris.eddins@jhuapl.edu.

ANGELA L. BARRIOS earned B.S., M.S., and Ph.D. degrees in aerospace engineering in 1993, 1995, and 1996, respectively, from Virginia Polytechnic Institute and State University in Blacksburg, Virginia. While a student, she performed theoretical and experimental work on single plate interferometry and boundary layer stability in steady and unsteady turbine blade flows, both cooled and uncooled. She joined APL in 1996 as a postdoctoral fellow in RTDC's Physics and Modeling Group, where she investigated water wave mitigation. Dr. Barrios became a member of the Senior Professional Staff in 1998, joining the Aerospace Sciences Group. Her current research areas include the development of advanced ignition concepts within scramjet combustors, advanced optical instrumentation development for missile lethality assessment, and algorithm development for missile typing and tracking. She is currently pursuing an M.S. in electrical engineering from The Johns Hopkins University in digital and communications signal processing. Her e-mail address is angela.barrios@jhuapl.edu.

DALE E. CLEMONS is a member of APL's Senior Professional Staff and an engineer in RTDC's Aeronautical Science and Technology Group. He received a B.S. in mechanical engineering from the University of Maryland, Baltimore County, in 1991, and an M.S. in mechanical engineering from The Johns Hopkins University Whiting School of Engineering in 1996. Since joining APL in 1992, Mr. Clemons has worked on design, analysis, and testing efforts in the Avery Advanced Technology Development Laboratory. He has also supported aerothermal/structural analysis efforts related to supersonic vehicles. He is currently involved in operations at the AATDL and is working to characterize Blast Initiation Detector performance. He has a Professional Engineer's license and holds membership in ASME. His e-mail address is dale.clemons@jhuapl.edu.

ROBERT F. WALSH Jr. is a member of APL's Senior Professional Staff in RTDC's Aeronautical Science and Technology Group. He received a bachelor's degree in mechanical engineering from Old Dominion University in 1990. Mr. Walsh joined APL later that year and has been involved in the design, fabrication, and testing of advanced aerospace propulsion systems and unmanned air vehicles as well as instrumented targets for Theater Ballistic Missiles. He is currently working as an APL field representative at Raytheon Missile Systems in Tucson, Arizona. His e-mail address is robert.walsh@jhuapl.edu.